High-K isomers in transactinide nuclei close to N=162

Prassa, Vaia; Lu, Bing-Nan; Nikšić, Tamara; Ackermann, D.; Vretenar, Dario

High-K isomers in transactinide nuclei close to $N = 162$

V. Prassa,[1] Bing-Nan Lu,[2] T. Nikšić,[1] D. Ackermann,[3] and D. Vretenar[1]
[1]*Physics Department, Faculty of Science, University of Zagreb, 10000 Zagreb, Croatia*
[2]*Institut fur Kernphysik, Institute for Advanced Simulation, and Jülich Center for Hadron Physics, Forschungszentrum Jülich, D-52425 Jülich, Germany*
[3]*GSI Helmholtzzentrum für Schwerionenforschung GmbH, Planckstrasse 1, 64291 Darmstadt, Germany*
(Received 14 January 2015; revised manuscript received 2 March 2015; published 23 March 2015)

We extend our recent study of shape evolution, collective excitation spectra, and decay properties of transactinide nuclei [V. Prassa, T. Nikšić, and D. Vretenar, Phys. Rev. C **88**, 044324 (2013)], based on the microscopic framework of relativistic energy density functionals, to two-quasiparticle (2qp) excitations in the axially deformed Rf, Sg, Hs, and Ds isotopes, with neutron number $N = 160$–166. The evolution of high-K isomers is analyzed in a self-consistent axially symmetric relativistic Hartree-Bogoliubov calculation using the blocking approximation with time-reversal symmetry breaking. The occurrence of a series of low-energy high-K isomers is predicted, in particular the 9^-_ν in the $N = 160$ and $N = 166$ isotopes, and the 12^-_ν in the $N = 164$ nuclei. The effect of the $N = 162$ deformed-shell closure on the excitation of 2qp states is discussed. In the $N = 162$ isotones we find a relatively low density of 2qp states, with no two-neutron states below 1.6 MeV excitation energy and two-proton states at ≈0.5 MeV higher energy than the lowest 2qp states in neighboring isotopes. This is an interesting result that can be used to characterise the occurrence of deformed shell gaps in very heavy nuclei.

DOI: 10.1103/PhysRevC.91.034324 PACS number(s): 21.60.Jz, 21.10.Gv, 21.10.Hw, 27.90.+b

I. INTRODUCTION

Relatively long-lived elements beyond the actinides owe their existence to the underlying single-nucleon shell structure. Nuclei in this region often display axially deformed equilibrium shapes and intruder single-nucleon states with high-Ω values (projection of the single-particle angular momentum onto the symmetry axis of the nucleus) appear close to the Fermi level. The unpaired quasiparticle excitations form isomeric states with high values of total $K = \Sigma_i \Omega_i$ [2]. Because they can only decay by K-forbidden transitions, these states have lifetimes that are significantly longer than most of the neighboring states. The decay of isomeric states provides information on the nuclear wave function, single-nucleon states, pairing gaps, and residual interactions [3]. Systematic experimental efforts in the region of very heavy nuclei have produced detailed spectroscopic data in nuclei around ^{254}No [4–8]. In addition to the detection of α and γ decays, recent studies have made use of conversion electrons (CE) to investigate possible K-isomeric states in heavy high-Z nuclei such as, for instance, ^{256}Rf, in which internal conversion becomes the preferred decay mode [9,10]. The heaviest nuclei for which characteristic high-K isomeric decays have been investigated are ^{270}Ds and its α-decay daughter ^{266}Hs [11,12].

Theoretical studies of quasiparticle excitations in the region of transactinide nuclei have been based on the microscopic-macroscopic approach [13–24], self-consistent models with Skyrme functionals [25–30], the Gogny force [31–33], and relativistic energy density functionals [1,34–38].

In the study of Ref. [1] we used a microscopic theoretical framework based on relativistic energy density functionals (REDFs) to analyze shape evolution, collective excitation spectra, and decay properties of transactinide nuclei. Axially symmetric and triaxial relativistic Hartree-Bogoliubov (RHB) calculations [36,39], based on the functional DD-PC1 [40] and with a separable pairing force of finite range [41,42], were carried out for the even-even isotopic chains between Fm and Fl. The occurrence of a deformed shell gap at neutron number $N = 162$ and its role on the stability of nuclei in the region around $Z = 108$ was investigated. A quadrupole collective Hamiltonian, with parameters determined by self-consistent constrained triaxial RHB calculations, was used to examine low-energy spectra of No, Rf, Sg, Hs, and Ds with neutron number in the interval $158 \leqslant N \leqslant 170$. In particular, we explored the isotopic dependence of several observables that characterize the transitions between axially symmetric rotors, γ-soft rotors, and spherical vibrators. The ratio $R_{4/2}$ of excitation energies of the yrast states 4^+_1 and 2^+_1, the ratio of reduced transition probabilities $R = B(E2; 4^+_1 \rightarrow 2^+_1)/B(E2; 2^+_1 \rightarrow 0^+_1)$, $B(E2)$ values for transitions within the ground-state band, and the level of K-mixing as reflected in the energy staggering between odd- and even-spin states in the (quasi-)γ bands, clearly show that all five isotopic chains display minimal variation from the axial rigid-rotor limit in the interval $N = 158$–166. For neutron numbers $N \geqslant 168$ their potential energy surfaces become more γ-soft. This is also reflected in the characteristic observables of rotational spectra.

As an illustration, in Fig. 1 we plot the self-consistent triaxial RHB energy surfaces in the β-γ plane ($0^\circ \leqslant \gamma \leqslant 60^\circ$) for ^{268,270,272,274}Hs ($Z = 108$). For each nucleus energies are normalized with respect to the binding energy of the equilibrium deformation. The color code refers to the energy at each point on the surface relative to the minimum. Details of the calculation and the choice of effective interactions in the particle-hole (DD-PC1 [40]) and particle-particle (a pairing force separable in momentum space [41,42]) channels, are given in Refs. [1,35]. The energy surfaces of Hs isotopes,

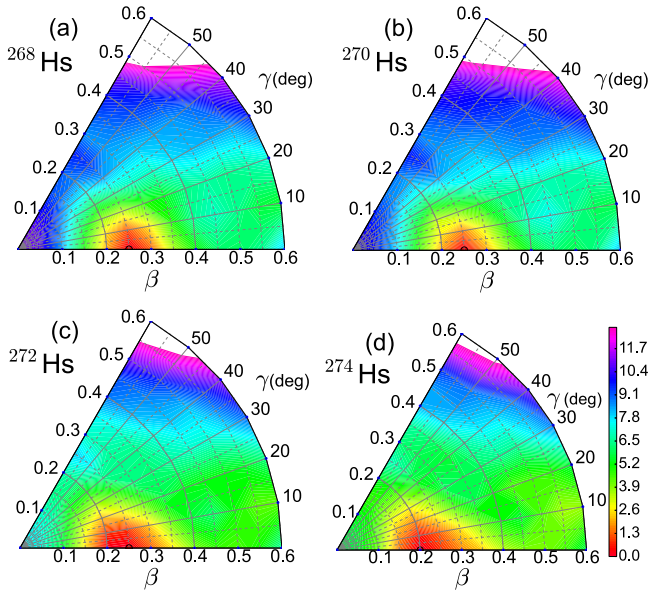

FIG. 1. (Color online) Self-consistent RHB triaxial energy maps of even-even Hs isotopes in the β-γ plane ($0^\circ \leqslant \gamma \leqslant 60^\circ$). For each nucleus energies are normalized with respect to the binding energy of the absolute minimum.

already reported in [1], display pronounced prolate axial minima ($\gamma \approx 0^\circ$) near $N = 162$, and the evolution of γ-softness with increasing neutron number.

II. TWO-QUASIPARTICLE EXCITATIONS IN AXIALLY DEFORMED TRANSACTINIDES

The occurrence of isomeric states based on single-nucleon Nilsson orbitals, and characterized by the projection K of the total angular momentum on the symmetry axis, is associated with axially symmetric shapes and, in even-even nuclei, these states are formed through broken-pair (two-quasiparticle or four-quasiparticle) excitations [3]. In the present study, therefore, we extend the analysis of constrained mean-field energy surfaces and collective excitation spectra of Ref. [1], to two-quasiparticle excitations in the axially deformed isotopes of Rf ($Z = 104$), Sg ($Z = 106$), Hs ($Z = 108$), and Ds ($Z = 110$), with neutron number $N = 160$–166. We are particularly interested in the occurrence of high-K isomers and the effect of the $N = 162$ closure on the structure and distribution of two-quasiparticle (2qp) states.

Two-quasiparticle neutron or proton states are obtained in a self-consistent RHB calculation using the blocking approximation. Axially symmetric solutions are assumed but the calculation includes time-reversal symmetry breaking. The 2qp states are determined by blocking the lowest neutron or proton quasiparticle orbitals located in the vicinity of the Fermi energy that corresponds to the fully paired equilibrium solution. After performing the iterative minimization, the energy of the two-quasiparticle excitation is obtained as the difference between the energy of the self-consistent blocked RHB solution and the energy of the fully paired equilibrium minimum. The breaking of time-reversal symmetry removes

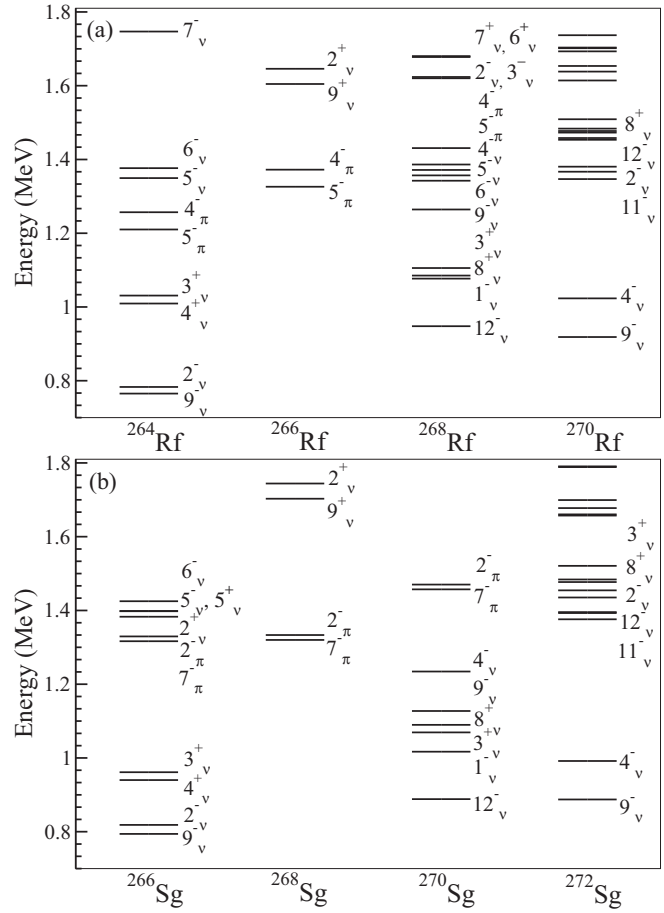

FIG. 2. Lowest two-quasiparticle states in Rf (upper panel) and Sg (lower panel) isotopes with neutron number $N = 160$–166. The 2qp states correspond to axially symmetric solutions obtained with the relativistic functional DD-PC1 and a pairing force separable in momentum space. The calculation includes time-reversal symmetry breaking.

the degeneracy between signature partner states with angular-momentum projection on the symmetry axis $K_{\min} = |\Omega_i - \Omega_j|$ and $K_{\max} = \Omega_i + \Omega_j$, and with parity $\pi = \pi_i \pi_j$.

Figures 2 and 3 display the excitation energies of two-quasiparticle $K_{\nu(\pi)}$ states for the Rf, Sg, Hs, and Ds isotopes with neutron number $N = 160$–166. The high density of single-particle levels close to the Fermi surface in ^{264}Rf yields a number of quasiparticle excitations in the energy window below 1.8 MeV. Our calculation predicts the occurrence of the two-neutron isomeric states $K^\pi = 9^-_\nu$ and 2^-_ν at energies 0.76 MeV and 0.78 MeV, respectively, originating from the single-particle orbitals $\nu 7/2^+[613] \otimes \nu 11/2^-[725]$. The neutron orbitals $\nu 1/2^+[620]$ and $\nu 7/2^+[613]$ are coupled to form the states 4^+_ν and 3^+_ν at excitation energy close to 1 MeV. The proton 2qp states 5^-_π and 4^-_π occur at 1.21 MeV and 1.26 MeV, respectively, and correspond to the configuration $\pi 1/2^-[521] \otimes \pi 9/2^+[624]$. An interesting result, that can also be noticed in the three other isotopic chains considered in this study, is that the lowest two-quasiparticle states in the $N = 162$ isotones are predicted at considerably higher excitation energies. For the particular choice of the energy

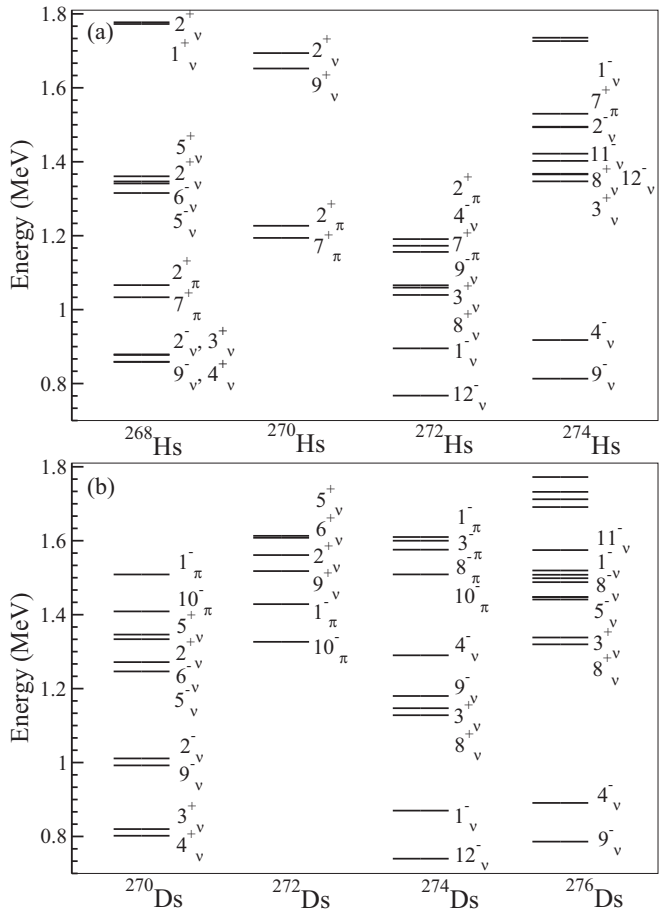

FIG. 3. Same as described in the caption to Fig. 2 but for the isotopes of Hs (upper panel) and Ds (lower panel).

density functional and pairing interaction used in this and our previous study [1], the lowest two-quasiparticle states typically occur at ≈0.8 MeV, whereas in the $N = 162$ isotones the excitation energies of the lowest 2qp states are predicted at $E \geqslant 1.2$ MeV. For ^{266}Rf, in particular, the doublet of states 5^-_π and 4^-_π states at energy 1.35 MeV originates from the two-proton configuration $\pi 1/2^-[521] \otimes \pi 9/2^+[624]$. The lowest two-neutron excitations occur at even higher energies: the 9^+_ν and 2^+_ν states at 1.60 MeV and 1.65 MeV, respectively, based on the high-j configuration $\nu 7/2^+[613] \otimes \nu 11/2^+[606]$. The occurrence of 2qp excitations in ^{268}Rf already at energies ≈1 MeV is consistent with the increase of the single-particle level density near the Fermi surface. The lowest-lying two-neutron excitations 12^-_ν and 1^-_ν are calculated at 0.95 and 1.08 MeV, respectively, and originate from the configuration $\nu 13/2^-[716] \otimes \nu 11/2^+[606]$. Blocking the orbitals $\nu 13/2^-[716]$ and $\nu 5/2^+[613]$ in ^{270}Rf ($N = 166$), yields the lowest high-K isomeric state 9^-_ν and the state 4^-_ν, at $E = 0.92$ and 1.02 MeV, respectively.

The lowest calculated two-quasiparticle isomers in Rf, Sg, Hs, and Ds isotopes are also listed in Table I in order of increasing excitation energies, together with the corresponding Nilsson configurations. Similarly to its isotone ^{264}Rf, in ^{266}Sg the lowest lying two-quasiparticle excitations are the 9^-_ν and 2^-_ν, at 0.79 and 0.81 MeV, respectively, followed by 4^+_ν at 0.94 MeV and 3^+_ν at 0.96 MeV. In ^{268}Sg, as a result of the neutron shell closure at $N = 162$, the lowest 2qp excitations are the proton states 7^-_π and 2^-_π at 1.32 and 1.33 MeV, respectively, originating from the Nilsson levels $\pi 5/2^-[512]$ and $\pi 9/2^+[624]$. We note that for this nucleus the only two-neutron qp states, predicted below 1.8 MeV are the 9^+_ν and 2^+_ν ($\nu 11/2^+[606] \otimes \nu 7/2^+[613]$) at 1.70 and 1.74 MeV, respectively. The lowest 2qp state in ^{270}Sg is the high-K isomer 12^-_ν which, together with the partner state 1^-_ν, has its origin in the high-j orbitals $\nu 11/2^+[606]$ and $\nu 13/2^-[716]$. At slightly higher excitation energies we find the sequence of states 8^+_ν and 3^+_ν ($\nu 5/2^+[613]$, $\nu 11/2^+[606]$), followed by 9^-_ν and 4^-_ν ($\nu 5/2^+[613]$, $\nu 13/2^-[716]$). In ^{272}Sg the lowest 2qp configurations are $\nu 5/2^+[613] \otimes \nu 13/2^-[716]$ (9^-_ν and 4^-_ν), $\nu 9/2^+[604] \otimes \nu 13/2^-[716]$ (11^-_ν and 2^-_ν), $\nu 11/2^+[606] \otimes \nu 13/2^-[716]$ (12^-_ν and 1^-_ν), and $\nu 5/2^+[613] \otimes \nu 11/2^+[606]$ (8^+_ν and 3^+_ν).

In ^{268}Hs the lowest-lying 2qp excitations are the signature partner levels 9^-_ν, 2^-_ν and 4^+_ν, 3^+_ν. The two configurations coincide in energy, with the aligned Ω states at 0.86 MeV and the anti-aligned ones at 0.88 MeV. In ^{270}Hs, because of the deformed shell closure, the neutron two-quasiparticle states 9^+_ν and 2^+_ν are predicted at energies 1.65 and 1.69 MeV, respectively. The lowest-lying 2qp states calculated for ^{270}Hs are the proton excitations 7^+_π and 2^+_π, with the structure of Nilsson orbitals $\pi 5/2^-[512] \otimes \pi 9/2^-[505]$. Consistent with the results obtained for Rf and Sg isotopes, ^{272}Hs and ^{274}Hs exhibit an increased density of two-quasiparticle states at low excitation energies. The dominant high-j orbitals from which these 2qp states originate are the $\nu 13/2^-[716]$, $\nu 11/2^+[606]$, and $\nu 5/2^+[613]$. ^{270}Hs has been observed in the reaction ^{248}Cm(^{26}Mg, $4n$). However, because of the low production cross section and consequently low number of observed events (three), no detailed spectroscopic data are available except for α decay energies and decay times [43].

Adding two more protons, the doublet 4^+_ν and 3^+_ν ($\nu 1/2^+[620] \otimes \nu 7/2^+[613]$) becomes the lowest 2qp excitation in the nucleus ^{270}Ds, at energy ≈0.8 MeV. The partner levels 9^-_ν and 2^-_ν, which are the lowest 2qp states in the $N = 160$ Rf, Sg, and Hs isotopes, are calculated ≈200 keV higher in energy. The prediction of a high-K two-neutron quasiparticle configuration at energy ≈1 MeV is in agreement with the experimental observation of a two-neutron high-K isomeric decay in ^{270}Ds [11]. The calculation for ^{272}Ds predicts the proton two-quasiparticle states 10^-_π and 1^-_π at energies 1.33 and 1.43 MeV, respectively, based on the configuration $\pi 9/2^-[505] \otimes \pi 11/2^+[615]$. Because of the $N = 162$ deformed shell gap the two-neutron doublets 9^+_ν, 2^+_ν and 5^+_ν, 6^+_ν, appear only at higher excitation energies (1.5 MeV). ^{272}Ds is the α-decay daughter of ^{276}Cn, which could be produced in a similar way as ^{270}Ds [11] via the reaction ^{207}Pb(^{70}Sn, $1n$)^{276}Cn. An order of magnitude lower production cross section could be compensated by higher beam intensities at future linear accelerator facilities, e.g., the LINAG project presently under construction for SPIRAL2 [44], or the project for a high-intensity continuous wave machine at GSI [45]. In ^{274}Ds and ^{276}Ds the density of 2qp excitations is evidently enhanced, reflecting the increased number of neutron

TABLE I. Lowest calculated two-quasiparticle isomers in Rf, Sg, Hs, and Ds isotopes with neutron number $N = 160$–166. For a given configuration of Nilsson orbitals breaking of time-reversal symmetry removes the degeneracy between signature partner states with angular-momentum projection on the symmetry axis $K_{\min} = |\Omega_1 - \Omega_2|$ and $K_{\max} = \Omega_1 + \Omega_2$.

Nucleus	Configuration	$K = \Omega_1 + \Omega_2$		$K = \|\Omega_1 - \Omega_2\|$	
		K^π	E (MeV)	K^π	E (MeV)
^{264}Rf	$\nu 7/2^+[613] \otimes \nu 11/2^-[725]$	9^-_ν	0.76	2^-_ν	0.78
	$\nu 7/2^+[613] \otimes \nu 1/2^+[620]$	4^+_ν	1.01	3^+_ν	1.03
	$\pi 1/2^-[521] \otimes \pi 9/2^+[624]$	5^-_π	1.21	4^-_π	1.26
^{266}Rf	$\pi 1/2^-[521] \otimes \pi 9/2^+[624]$	5^-_π	1.33	4^-_π	1.37
	$\nu 7/2^+[613] \otimes \nu 11/2^+[606]$	9^+_ν	1.60	2^+_ν	1.65
^{268}Rf	$\nu 13/2^-[716] \otimes \nu 11/2^+[606]$	12^-_ν	0.95	1^-_ν	1.08
	$\nu 5/2^+[613] \otimes \nu 11/2^+[606]$	8^+_ν	1.09	3^+_ν	1.11
	$\nu 5/2^+[613] \otimes \nu 13/2^-[716]$	9^-_ν	1.26	4^-_ν	1.37
	$\nu 1/2^-[750] \otimes \nu 11/2^+[606]$	6^-_ν	1.34	5^-_ν	1.36
	$\pi 1/2^-[521] \otimes \pi 9/2^+[624]$	5^-_π	1.39	4^-_π	1.43
^{270}Rf	$\nu 13/2^-[716] \otimes \nu 5/2^+[613]$	9^-_ν	0.92	4^-_ν	1.02
	$\nu 9/2^+[604] \otimes \nu 13/2^-[716]$	11^-_ν	1.35	2^-_ν	1.37
	$\nu 11/2^+[606] \otimes \nu 13/2^-[716]$	12^-_ν	1.38	1^-_ν	1.51
	$\nu 5/2^+[613] \otimes \nu 11/2^+[606]$	8^+_ν	1.45	3^+_ν	1.47
	$\nu 3/2^+[611] \otimes \nu 13/2^-[716]$	8^-_ν	1.48	5^-_ν	1.48
^{266}Sg	$\nu 7/2^+[613] \otimes \nu 11/2^-[725]$	9^-_ν	0.79	2^-_ν	0.81
	$\nu 7/2^+[613] \otimes \nu 1/2^+[620]$	4^+_ν	0.94	3^+_ν	0.96
	$\pi 5/2^-[512] \otimes \pi 9/2^+[624]$	7^-_π	1.32	2^-_π	1.33
^{268}Sg	$\pi 5/2^-[512] \otimes \pi 9/2^+[624]$	7^-_π	1.32	2^-_π	1.33
	$\nu 7/2^+[613] \otimes \nu 11/2^+[606]$	9^+_ν	1.70	2^+_ν	1.74
^{270}Sg	$\nu 13/2^-[716] \otimes \nu 11/2^+[606]$	12^-_ν	0.89	1^-_ν	1.02
	$\nu 5/2^+[613] \otimes \nu 11/2^+[606]$	8^+_ν	1.09	3^+_ν	1.07
	$\nu 5/2^+[613] \otimes \nu 13/2^-[716]$	9^-_ν	1.13	4^-_ν	1.23
	$\pi 5/2^-[512] \otimes \pi 9/2^+[624]$	7^-_π	1.46	2^-_π	1.47
^{272}Sg	$\nu 5/2^+[613] \otimes \nu 13/2^-[716]$	9^-_ν	0.89	4^-_ν	0.99
	$\nu 9/2^+[604] \otimes \nu 13/2^-[716]$	11^-_ν	1.38	2^-_ν	1.40
	$\nu 11/2^+[606] \otimes \nu 13/2^-[716]$	12^-_ν	1.39	1^-_ν	1.52
	$\nu 5/2^+[613] \otimes \nu 11/2^+[606]$	8^+_ν	1.44	3^+_ν	1.46
^{268}Hs	$\nu 7/2^+[613] \otimes \nu 11/2^-[725]$	9^-_ν	0.86	2^-_ν	0.88
	$\nu 7/2^+[613] \otimes \nu 1/2^+[620]$	4^+_ν	0.86	3^+_ν	0.88
	$\pi 5/2^-[512] \otimes \pi 9/2^-[505]$	7^+_π	1.03	2^+_π	1.07
^{270}Hs	$\pi 5/2^-[512] \otimes \pi 9/2^-[505]$	7^+_π	1.19	2^+_π	1.23
	$\nu 7/2^+[613] \otimes \nu 11/2^+[606]$	9^+_ν	1.65	2^+_ν	1.69
^{272}Hs	$\nu 11/2^+[606] \otimes \nu 13/2^-[716]$	12^-_ν	0.77	1^-_ν	0.89
	$\nu 5/2^+[613] \otimes \nu 11/2^+[606]$	8^+_ν	1.04	3^+_ν	1.06
	$\nu 5/2^+[613] \otimes \nu 13/2^-[716]$	9^-_ν	1.07	4^-_ν	1.17
	$\pi 5/2^-[512] \otimes \pi 9/2^-[505]$	7^+_π	1.16	2^+_π	1.19
^{274}Hs	$\nu 5/2^+[613] \otimes \nu 13/2^-[716]$	9^-_ν	0.81	4^-_ν	0.92
	$\nu 5/2^+[613] \otimes \nu 11/2^+[606]$	8^+_ν	1.37	3^+_ν	1.35
	$\nu 11/2^+[606] \otimes \nu 13/2^-[716]$	12^-_ν	1.37	1^-_ν	1.49
	$\nu 9/2^+[604] \otimes \nu 13/2^-[716]$	11^-_ν	1.40	2^-_ν	1.42
^{270}Ds	$\nu 7/2^+[613] \otimes \nu 1/2^+[620]$	4^+_ν	0.80	3^+_ν	0.82
	$\nu 7/2^+[613] \otimes \nu 11/2^-[725]$	9^-_ν	0.99	2^-_ν	1.01
	$\nu 1/2^+[620] \otimes \nu 11/2^-[725]$	6^-_ν	1.27	5^-_ν	1.25
^{272}Ds	$\pi 9/2^-[505] \otimes \pi 11/2^+[615]$	10^-_π	1.33	1^-_π	1.43
	$\nu 7/2^+[613] \otimes \nu 11/2^+[606]$	9^+_ν	1.52	2^+_ν	1.56
	$\nu 1/2^+[620] \otimes \nu 11/2^+[606]$	6^+_ν	1.61	5^+_ν	1.61
^{274}Ds	$\nu 11/2^+[606] \otimes \nu 13/2^-[716]$	12^-_ν	0.74	1^-_ν	0.87
	$\nu 5/2^+[613] \otimes \nu 11/2^+[606]$	8^+_ν	1.13	3^+_ν	1.15
	$\nu 5/2^+[613] \otimes \nu 13/2^-[716]$	9^-_ν	1.18	4^-_ν	1.29
	$\pi 9/2^-[505] \otimes \pi 11/2^+[615]$	10^-_π	1.51	1^-_π	1.61
	$\pi 11/2^+[615] \otimes \nu 5/2^-[512]$	8^-_π	1.58	3^-_π	1.60

TABLE I. (*Continued.*)

Nucleus	Configuration	$K = \Omega_1 + \Omega_2$		$K = \lvert\Omega_1 - \Omega_2\rvert$	
		K^π	E (MeV)	K^π	E (MeV)
^{276}Ds	$\nu 5/2^+[613] \otimes \nu 13/2^-[716]$	9^-_ν	0.79	4^-_ν	0.89
	$\nu 5/2^+[613] \otimes \nu 11/2^+[606]$	8^+_ν	1.33	3^+_ν	1.35
	$\nu 3/2^+[611] \otimes \nu 13/2^-[716]$	8^-_ν	1.45	5^-_ν	1.44
	$\nu 11/2^+[606] \otimes \nu 13/2^-[716]$	12^-_ν	1.58	1^-_ν	1.45
	$\nu 9/2^+[604] \otimes \nu 13/2^-[716]$	11^-_ν	1.49	2^-_ν	1.51
	$\pi 11/2^+[615] \otimes \pi 5/2^-[512]$	8^-_π	1.50	3^-_π	1.52

single-particle orbitals close to the Fermi surface. The lowest Nilsson levels that form the 2qp configurations in the energy window below 1.8 MeV are the $13/2^-[716]$, $11/2^+[606]$, $5/2^+[613]$, and $3/2^+[611]$ for neutrons, and the orbitals $11/2^+[615]$, $9/2^-[505]$, and $5/2^-[512]$ for protons.

III. CONCLUSIONS

In summary, we have employed the self-consistent mean-field framework based on relativistic energy density functionals to study the structure of two-quasiparticle excitations in axially deformed Rf, Sg, Hs, and Ds isotopes, with neutron number $N = 160$–166. The calculation of excitation energies of 2qp states is based on the blocking approximation with time-reversal symmetry breaking. In addition to a few already available data (an α-decaying isomer at $E_x \approx 1.13$ MeV in ^{270}Ds with a suggested two-neutron configuration [11], populates excited states in the daughter nucleus ^{266}Hs, among which one is an isomer [12]), in the near future one can expect more spectroscopic information on high-K isomeric states in the region of transactinide nuclei around $N = 162$. Our microscopic self-consistent calculation has provided a detailed prediction for the evolution of 2qp states close to the $N = 162$ deformed-shell gap. The excitation energies of 2qp configurations depend, in addition to the specific choice of the energy density functional, also on the strength of the pairing interaction. As in our recent study of shape evolution, collective excitation spectra, and decay properties of transactinide nuclei [1], in the particle-hole channel we have used the relativistic functional DD-PC1 that was adjusted to the experimental masses of a set of 64 axially deformed nuclei in the mass regions $A \approx 150$–180 and $A \approx 230$–250. The strength of the separable pairing force of finite range was fine-tuned to reproduce the odd-even mass differences in the region $A \approx 230$–250. A stronger (weaker) pairing would automatically increase (decrease) the energies of the 2qp states (shown in Figs. 2 and 3) with respect to the corresponding ground states. The calculation predicts the occurrence of a series of low-energy high-K isomers, most notably the 9^-_ν in the $N = 160$ and $N = 166$ isotopes, and the 12^-_ν in the $N = 164$ nuclei. A very interesting result is the low density of 2qp states in the $N = 162$ isotones, with no two-neutron states predicted below 1.6 MeV excitation energy. The two-proton states in these nuclei are calculated almost 0.5 MeV higher in energy than the lowest 2qp states in neighboring isotopes. This is a consequence of the deformed-shell closure at $N = 162$ and presents an interesting observable that can be used, together with the separation energies and Q_α values, to characterize the evolution of deformed shell gaps in this mass region, and possibly verified experimentally in the near future for ^{270}Hs and ^{272}Ds.

ACKNOWLEDGMENTS

This work has been supported by the NEWFELPRO project of Ministry of Science, Croatia, co-financed through the Marie Curie FP7-PEOPLE-2011-COFUND program. B.-N.L. and D.V. acknowledge the support of the Helmholtz-Institut Mainz.

[1] V. Prassa, T. Nikšić, and D. Vretenar, Phys. Rev. C **88**, 044324 (2013).
[2] K. E. G. Löbner, Phys. Lett. B **26**, 369 (1968).
[3] P. M. Walker and G. D. Dracoulis, Nature **399**, 35 (1999).
[4] R.-D. Herzberg and P. T. Greenlees, Prog. Part. Nucl. Phys. **61**, 674 (2008).
[5] R.-D. Herzberg and D. M. Cox, Radiochim. Acta **99**, 441 (2011).
[6] P. T. Greenlees *et al.*, Phys. Rev. Lett. **109**, 012501 (2012).
[7] B. Sulignano *et al.*, Phys. Rev. C **86**, 044318 (2012).
[8] J. Rissanen *et al.*, Phys. Rev. C **88**, 044313 (2013).
[9] H. B. Jeppesen *et al.*, Phys. Rev. C **79**, 031303(R) (2009).
[10] A. P. Robinson *et al.*, Phys. Rev. C **83**, 064311 (2011).
[11] S. Hofmann *et al.*, Eur. Phys. J. A **10**, 5 (2001).
[12] D. Ackermann *et al.*, GSI Sci. Rep. **2011**, 208 (2012); (to be published).
[13] S. Nilsson, J. Nix, A. Sobiczewski, Z. Szymański, S. Wycech, C. Gustafson, and P. Möller, Nucl. Phys. A **115**, 545 (1968).
[14] A. Sobiczewski, I. Muntian, and Z. Patyk, Phys. Rev. C **63**, 034306 (2001).
[15] A. Sobiczewski and K. Pomorski, Prog. Part. Nucl. Phys. **58**, 292 (2007).
[16] A. Sobiczewski, Radiochim. Acta **99**, 395 (2011).
[17] G. G. Adamian, N. V. Antonenko, and W. Scheid, Phys. Rev. C **81**, 024320 (2010).
[18] A. N. Kuzmina, G. G. Adamian, and N. V. Antonenko, Phys. Rev. C **85**, 027308 (2012).

[19] F. R. Xu, E. G. Zhao, R. Wyss, and P. M. Walker, Phys. Rev. Lett. **92**, 252501 (2004).
[20] D. S. Delion, R. J. Liotta, and R. Wyss, Phys. Rev. C **76**, 044301 (2007).
[21] H. L. Liu, F. R. Xu, P. M. Walker, and C. A. Bertulani, Phys. Rev. C **83**, 011303(R) (2011).
[22] H. L. Liu, F. R. Xu, and P. M. Walker, Phys. Rev. C **86**, 011301(R) (2012).
[23] H. L. Liu and F. R. Xu, Phys. Rev. C **87**, 067304 (2013).
[24] H. L. Liu, P. M. Walker, and F. R. Xu, Phys. Rev. C **89**, 044304 (2014).
[25] S. Ćwiok, J. Dobaczewski, P.-H. Heenen, P. Magierski, and W. Nazarewicz, Nucl. Phys. A **611**, 211 (1996).
[26] S. Ćwiok, W. Nazarewicz, and P. H. Heenen, Phys. Rev. Lett. **83**, 1108 (1999).
[27] T. Duguet, P. Bonche, and P.-H. Heenen, Nucl. Phys. A **679**, 427 (2001).
[28] M. Bender, P. Bonche, T. Duguet, and P.-H. Heenen, Nucl. Phys. A **723**, 354 (2003).
[29] M. Bender and P.-H. Heenen, J. Phys.: Conf. Ser. **420**, 012002 (2013).
[30] Yue Shi, J. Dobaczewski, and P. T. Greenlees, Phys. Rev. C **89**, 034309 (2014).
[31] J. L. Egido and L. M. Robledo, Phys. Rev. Lett. **85**, 1198 (2000).
[32] J.-P. Delaroche, M. Girod, H. Goutte, and J. Libert, Nucl. Phys. A **771**, 103 (2006).
[33] M. Warda and J. L. Egido, Phys. Rev. C **86**, 014322 (2012).
[34] A. V. Afanasjev, T. L. Khoo, S. Frauendorf, G. A. Lalazissis, and I. Ahmad, Phys. Rev. C **67**, 024309 (2003).
[35] V. Prassa, T. Nikšić, G. A. Lalazissis, and D. Vretenar, Phys. Rev. C **86**, 024317 (2012).
[36] D. Vretenar, A. V. Afanasjev, G. Lalazissis, and P. Ring, Phys. Rep. **409**, 101 (2005).
[37] E. Litvinova, Phys. Rev. C **85**, 021303(R) (2012).
[38] A. V. Afanasjev and O. Abdurazakov, Phys. Rev. C **88**, 014320 (2013).
[39] J. Meng, H. Toki, S. G. Zhou, S. Q. Zhang, W. H. Long, and L. S. Geng, Prog. Part. Nucl. Phys. **57**, 470 (2006).
[40] T. Nikšić, D. Vretenar, and P. Ring, Phys. Rev. C **78**, 034318 (2008).
[41] Y. Tian, Z. Y. Ma, and P. Ring, Phys. Lett. B **676**, 44 (2009).
[42] T. Nikšić, P. Ring, D. Vretenar, Y. Tian, and Z. Y. Ma, Phys. Rev. C **81**, 054318 (2010).
[43] J. Dvorak *et al.*, Phys. Rev. Lett. **97**, 242501 (2006).
[44] R. Ferdinand, *Proceedings of the 5th International Particle Accelerator Conference IPAC2014, Dresden, Germany* (2014), p. 1852, http://hal.in2p3.fr/in2p3-01009261v1.
[45] W. Barth, in [44], (2014), p. 3211.